ISSN 0020-4412, Instruments and Experimental Techniques, 2007, Vol. 50, No. 2, pp. 176–186. © Pleiades Publishing, Ltd., 2007.
Original Russian Text © A.G. Voronin, V.M. Grebenyuk, D.E. Karmanov, N.A. Korotkova, Z.V. Krumshtein, M.M. Merkin, A.Yu. Pakhomov, D.M. Podorozhnyi, A.B. Sadovskii, L.G. Sveshnikova, L.G. Tkachev, A.N. Turundaevskii, 2007, published in Pribory i Tekhnika Eksperimenta, 2007, No. 2, pp. 39–49.

NUCLEAR EXPERIMENTAL TECHNIQUE

Testing the Prototype of the NUCLEON Setup on the Pion Beam of the SPS Accelerator (CERN)

A. G. Voronin[a], V. M. Grebenyuk[b], D. E. Karmanov[a], N. A. Korotkova[a], Z. V. Krumshtein[b], M. M. Merkin[a], A. Yu. Pakhomov[a], D. M. Podorozhnyi[a], A. B. Sadovskii[b], L. G. Sveshnikova[a], L. G. Tkachev[b], and A. N. Turundaevskii[a]

[a] *Skobel'tsyn Institute of Nuclear Physics, Moscow State University, Vorob'evy gory 1, str. 2, Moscow, 119992 Russia*

[b] *Joint Institute for Nuclear Research, ul. Joliot-Curie 6, Dubna, Moscow oblast, 141980 Russia*

Received May 29, 2006; in final form, July 11, 2006

Abstract—A technique for determining the energy of primary cosmic rays in the range of 10^{12}–10^{15} eV has been developed. The idea behind this technique consists in measuring the spatial flux density of secondary particles produced in the first act of inelastic nuclear interaction inside a target and passed through a thin converter layer in which the electromagnetic component (photons from decays of neutral pions) is multiplied. This technique has been developed by generalizing the well-known Castagnoli method (for measuring the angular characteristics of tracks of secondary particles produced in the first act of inelastic nuclear interaction inside a target), and its application offers a chance to design instruments for scientific studies such that their mass is relatively low while their luminosity is high. It is proposed to use this technique in a satellite-based NUCLEON experiment. The technique has been tested on charged particle beams of the SPS accelerator at CERN. Results of these tests confirm that, using this method, it is possible to measure the particle energy and, therefore, perform an orbital scientific experiment with the proposed equipment.

PACS numbers: 29.30.Ep, 29.40.Gx, 96.50.sb

DOI: 10.1134/S0020441207020029

INTRODUCTION

To promote direct investigations of cosmic rays (CRs) in the high-energy region, a new approach to taking energy measurements—the kinematic lightweight energy meter (KLEM) technique—was proposed in [1, 2]. The idea of this technique is to measure the energy of a primary particle from the energy distribution of a flux of secondary particles produced in a thin target in the first act of inelastic interaction and multiplied in a tungsten converter. This technique offers a chance to design instruments for scientific studies such that their mass is relatively low while their luminosity is high and to carry out direct investigations of high-energy CRs in the range of 10^{14}–10^{15} eV. Based on the KLEM technique, a project of the NUCLEON space experiment aimed at studying the CRs in the region below the "knee" in the energy range of 10^{12}–10^{15} eV has been proposed. In the most interesting subrange of 10^{13}–10^{15} eV, the data available today are inconsistent and their statistical accuracy is insufficient.

This project has been supported by the Russian Academy of Sciences and included in the Russian Federal Space Research Program.

THE KLEM TECHNIQUE AND OBJECTIVES OF THE EXPERIMENT ON THE ACCELERATOR

Our approach for determining the energy of CR particles is essentially a combination of a technique for measuring the kinematic characteristics, which are sensitive to the Lorentz factor of a primary particle, and a thin calorimeter for measuring the energy converted into an electron–photon component.

The ordinary kinematic technique is based on measuring the fly-off angles of secondary particles produced in an act of inelastic interaction between a particle and an atomic nucleus in a target. In this case, Lorentz factor of the incident particle (which is directly related to particle energy E and mass m) $\gamma = E/m$ is defined as the mean logarithm of the tangent of exit angles θ_i for all secondary particles: $\ln(E/m) \sim \langle -\ln\tan\theta \rangle$. From this formula, it is apparent that the mean exit angle of secondary particles decreases with increasing energy and, therefore, the cascade becomes "narrower."

Instead of reconstructing the tracks of individual particles in the event under investigation, the KLEM technique implies measuring the spatial distribution of the density of secondary particles using microstrip detectors with a spatial resolution of 100–500 μm. The detectors are placed at distance H from the target, where the primary interaction vertex is located. The spatial distribution is characterized by parameter $S(E) = \sum \ln^2 \tan\theta_i/2$, which is sensitive both to the exit angles of particles and to their multiplicity. For the actual experiment, this parameter is $S = \sum \ln^2(2H/X_i)N_i$, where X_i is the distance from the strip to the shower axis, N_i is the total ionization loss proportional to the number of single-charged particles that hit the strip, and H is the distance from the target's center to the plane of the detectors.

The practical applicability of the proposed technique was estimated using the results of large-scale simulation [1] employing the GEANT 3.21 software package [3] complemented by the QGSJET nuclear interaction generator [4, 5], which provided a means to describe high-energy hadron–nucleus and nucleus–nucleus interactions. Different variants for the structure of the spectrometer operating according to the KLEM technique in a wide energy range were investigated.

Simulation showed that, when the KLEM technique is used, the energy dependence obeys power law $S \sim E^{\beta}$ over a wide range of energies (10^{11}–10^{16} eV) for all nuclei with Z = 1–30, index of power β being 0.74–0.82. The error in determining individual particle energy E is rather high, $\sigma(E)$ ~ 0.7–0.9. However, as was shown in [1], this error in measuring the descending CR spectrum ($F(E) \sim E^{-2.7}$) is considerably lower (~50%); therefore, this method can be used to measure the power spectrum of particles in the desired energy range.

This method provides a means to create an experimental setup with a relatively low mass and a high luminosity, which opens prospects for developing an orbital spectrometer with a long exposure time and carrying our investigations of CRs over a wide range of energies according to a unified technique.

To solve this physical problem, it is necessary that the particle charge and angle of incidence be measured, i.e., the particle trajectory in the chamber be reconstructed. In this case, the task is to distinguish a useful event—a particle with a threshold energy of 1 TeV that is of interest for us—from low-energy and out-of-aperture background events. All this requires careful testing of experimental procedures on extracted hadron and nuclear beams of the SPS accelerator at CERN. For the first time, the method was tested on an extracted pion beam in 2002 and demonstrated the feasibility of such an experiment [2].

In 2005, an additional experiment was conducted on the extracted pion beam with energies of 100–350 GeV.

The main objectives of the experiment on the accelerator were as follows:

(1) developing a procedure for calibrating the channels of the microstrip detectors;

(2) analyzing the accuracy of reconstructing the shower axis in the setup;

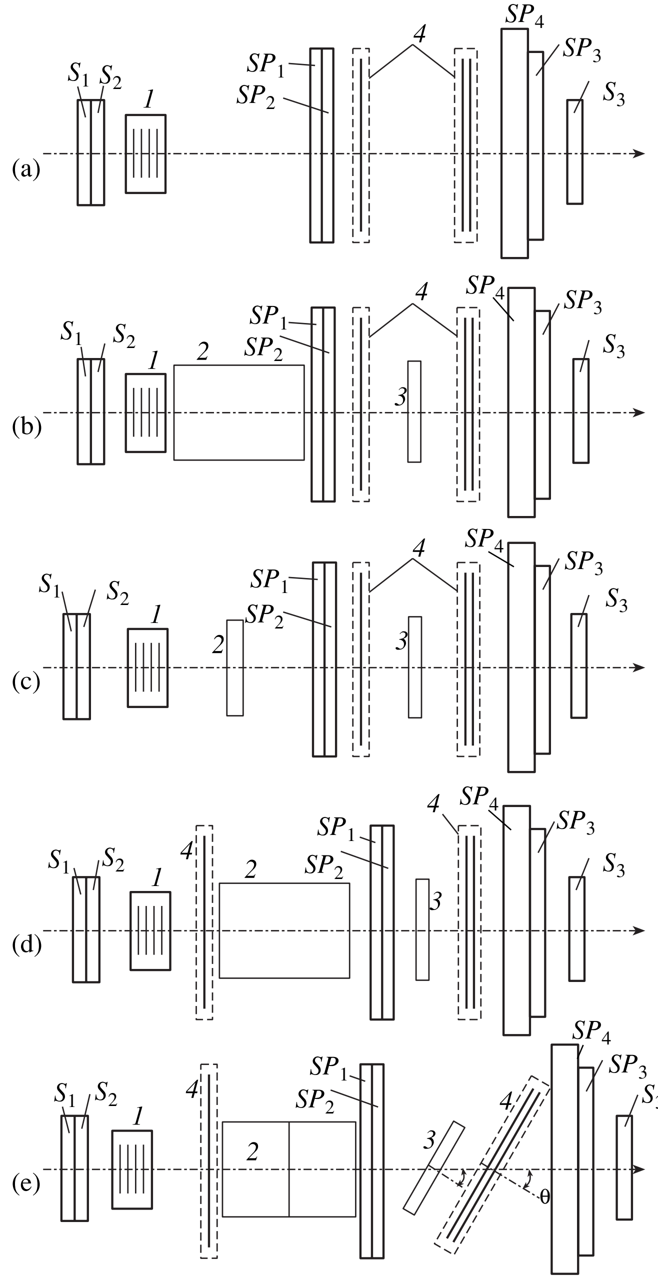

Fig. 1. Configurations of the setup prototypes adapted for performing different tasks of the experiment on the beam: (a) calibrating the channel, (b) testing the prototype that reproduces the configuration of the actual instrument (for investigating the accuracy of energy reconstruction) to the maximum extent, (c) localizing the first inelastic scattering, (d) for investigating the influence of the reverse current on the instrument, and (e) for studying angular events; (*1*) charge-measuring system, (*2*) target, (*3*) tungsten converter, (*4*) microstrip detectors, (S_1–S_3) trigger scintillation counters of the T2-H2 channel, and (SP_1–SP_4) prototypes of the trigger scintillation detectors.

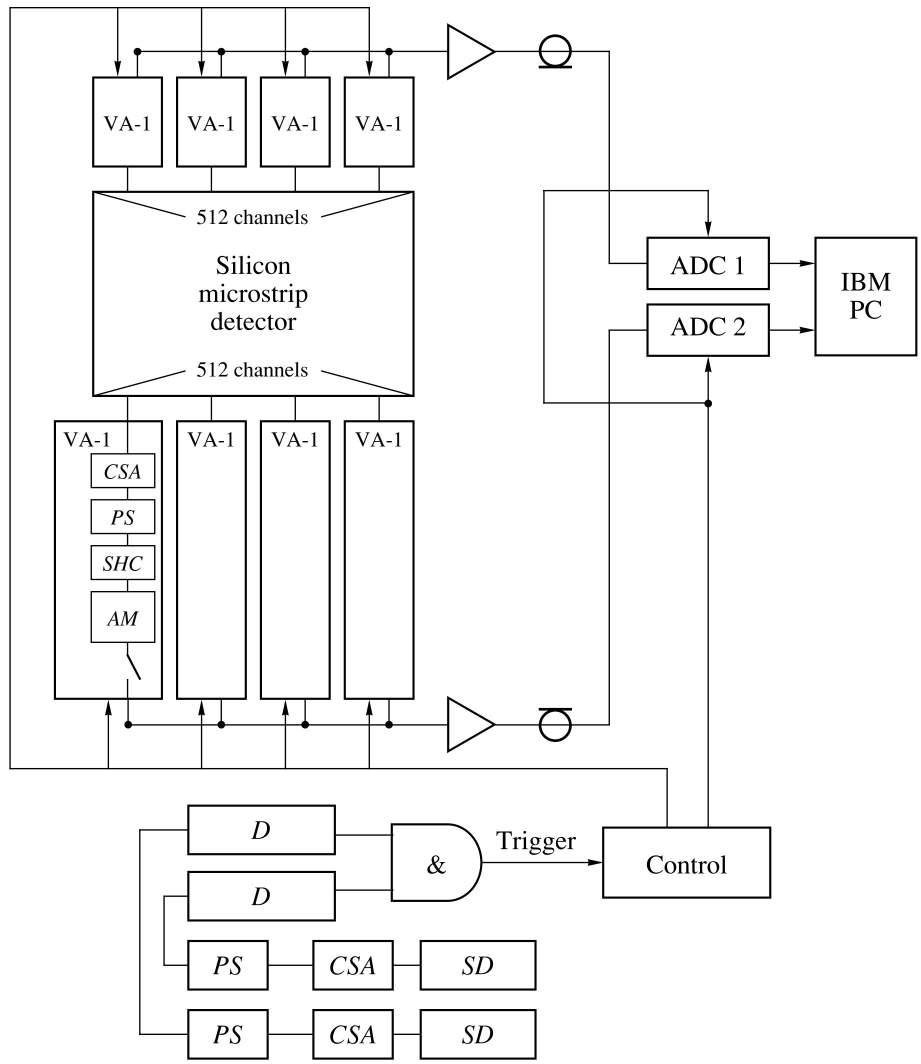

Fig. 2. Diagram of the electronic system of the setup: (*D*) discriminator, (*PS*) pulse shaper, (*CSA*) charge-sensitive amplifier, (*SD*) silicon detector, (*AM*) analog memory, and (*SHC*) sample-and-hold circuit.

(3) localizing the point of the first inelastic interaction;

(4) examining the energy reconstruction accuracy at different energies and incident angles and comparing it to the results of simulation; and

(5) investigating the trigger scintillation detectors.

The problem of accuracy in determining the particle charge was considered in [6].

PROTOTYPE OF THE NUCLEON SETUP

An experimental setup prototype has been developed such that the location of its components can be changed according to the objectives of each particular experiment. Figure 1 shows the configurations of the setup prototype that permit the performance of the above tasks. In the diagrams, we present the disposition of the trigger system.

The prototype of the setup contains charge-measuring system *1*, a system of microstrip silicon detectors *4*, and a fast trigger system based on scintillation counters S_1–S_3. A primary particle suffers nuclear interaction inside carbon target *2* 1–10 cm thick, producing secondary charged particles (mostly π^+ and π^-) and photons (from π^0 and η-meson decays). At some distance from the target there is tungsten layer *3* of changeable thickness, which converts photons into electron–positron pairs. A system of microstrip detectors, capable of measuring the distribution density of secondary charged particles, is located immediately behind the converter.

The charge-measuring system is composed of four arrays of silicon detectors, each of which is divided into separate pads. Information on the incident particle charge is independently collected from each array, thus providing a higher accuracy of measurements than is

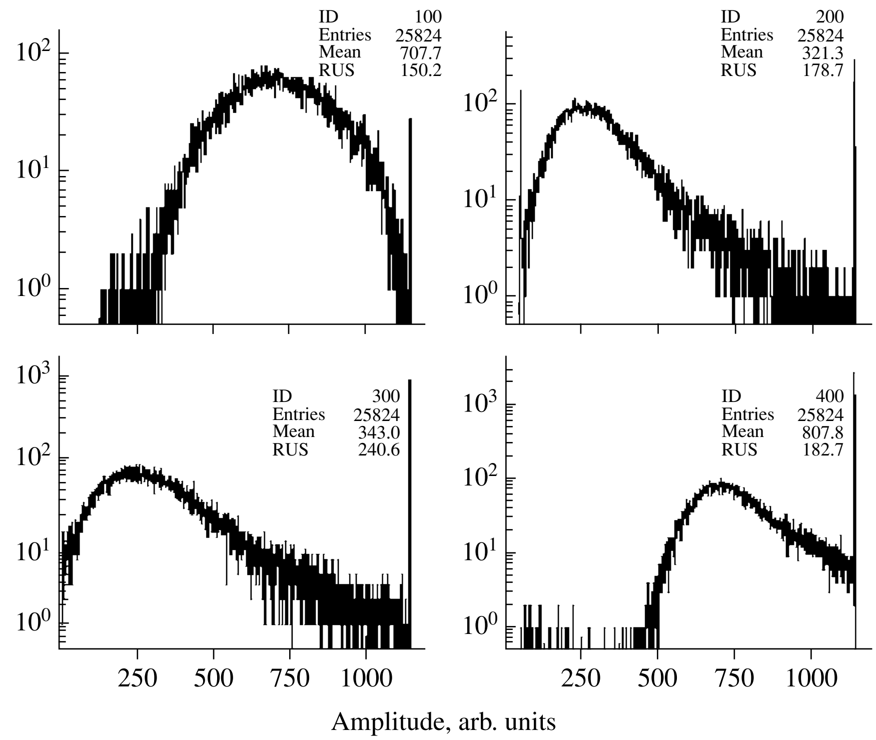

Fig. 3. Amplitude distributions for four planes of the trigger detectors. A peak corresponds to the signal from MIPs. Both a target and a converter were absent. The voltages applied to the PMTs were U_{SP_1} = 1620 V, U_{SP_2} = 1650 V, U_{SP_3} = 1780 V, and U_{S_3} = 1850 V.

achieved with a single array. The other destination of the charge-measuring system is to generate a trigger signal for the coordinate-measuring system, which is done using a coincidence circuit.

Four detector arrays of the charge-measuring system are enclosed in a common metal light-proof case having a thin window in the path of the beam; the separation between the arrays is 5 mm. A system of fasteners connects the case with the detectors to the bearing surface of the metal base on which a board with a reader is installed. The base with the reader and the detector unit is fixed on the bed in a movable mount of the dovetail type, which allows the unit to move in a horizontal direction in a plane perpendicular to the beam axis.

The microstrip detectors and the reader are mounted on a common board and housed in a case with windows covered by aluminum foil.

A supply voltage changer module, control signal splitter boards, and a switching unit are mounted on a separate base.

The signals from the charge-measuring unit and the system of microstrip detectors are converted into digital codes using two two-channel serial 12-bit ADCs built into an IBM PC-compatible computer and a special data acquisition program.

CHARACTERISTICS OF THE TEST BEAM IN THE SPS T2-H2 CHANNEL (CERN)

The T2-H2 channel of the SPS accelerator at CERN is a test channel; it is primarily used to test equipment of experimental facilities developed for the future LHC accelerator, as well as prototypes of other detectors, in particular, for astrophysical experiments. The versatility of the channel stems from the diversity of its beams: a negative pion beam with energies in the range of 150–350 GeV, an intensity as great as 10^6–10^7 particles/s, and a spill duration of ~1.6 s during slow extraction; proton and positive pion beams with the same parameters; and an electron beam with energies of 100–300 GeV. The NUCLEON equipment was mainly tested on a negative pion beam, which was the purest. The equipment tested in this run was incapable of operating at intensities greater than ~2×10^3 particles/spill.

DESCRIPTION OF THE DETECTORS AND THE DATA READOUT ELECTRONICS

The microstrip detector is produced from high-resistance *n*-type silicon 300 μm thick and contains 1024 strips separated by 50 μm. The dimensions of the sensitive zone are 51 × 50 mm. Each detector channel is connected to its own readout input. The charge detector is produced from high-resistance *p*-type silicon 400 μm thick and has an area of 10 cm^2. The setup contains four

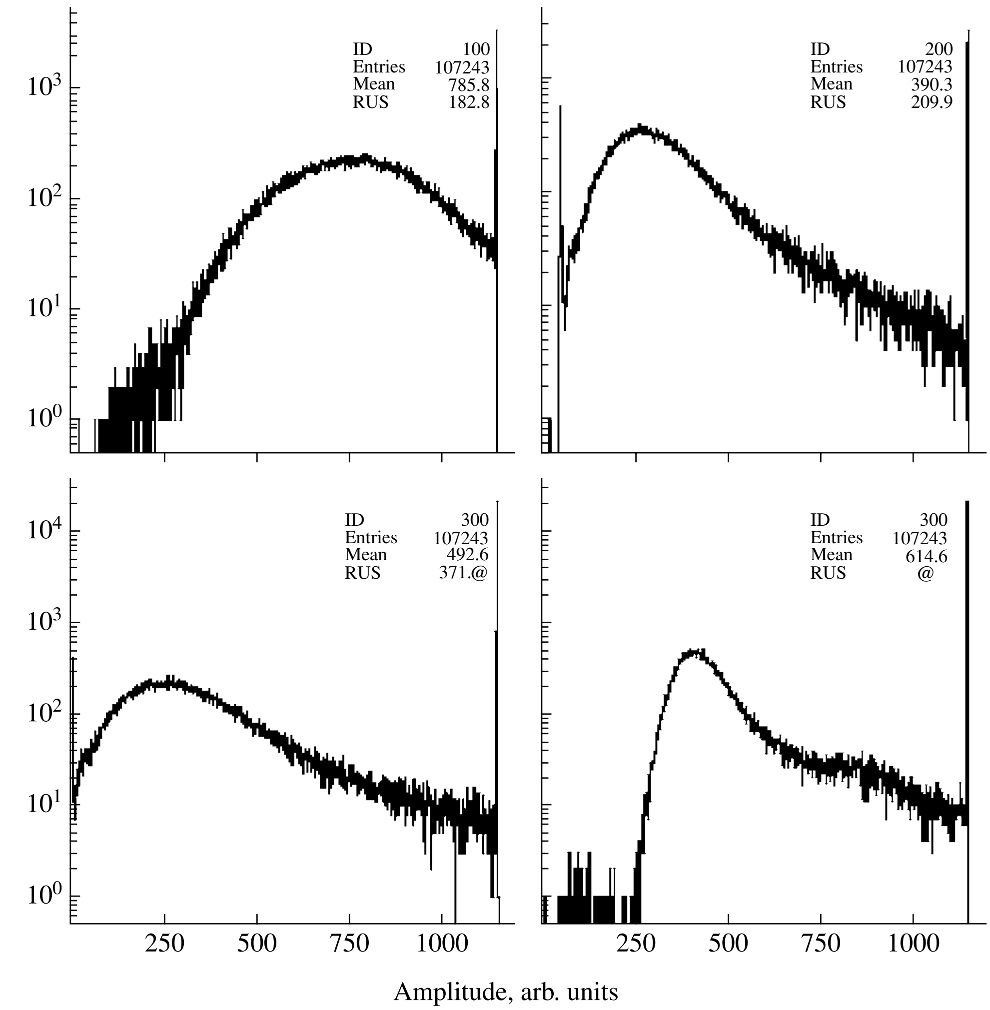

Fig. 4. Amplitude distributions for four planes of trigger detectors. The voltages applied to the PMTs were U_{SP_1} = 1620 V, U_{SP_2} = 1650 V, U_{SP_3} = 1780 V, and U_{S_3} = 1750 V. The target and the converter were 100 and 35 mm thick, respectively.

successive detectors, two of which are used to produce a trigger pulse for the data readout system. The four detectors act as a charge-measuring system, for which each detector has two measuring channels with different gains, as well as a fast trigger channel. Each of the three strip detector arrays contains one detector and eight 128-channel VA-1 chips (Viking) [7] used to read information out of each of 1024 strips. Each channel has a charge-sensitive preamplifier, a pulse shaper, a sample-and-hold circuit, and an analog switch. The diagram of the electronic system is shown in Fig. 2.

To produce a trigger, the detector signals were passed through the discriminator–shapers and fed into an AND/OR logic circuit. A trigger was generated when the signals arrived from both detectors. The thresholds of the trigger pulse generators were set at a level corresponding to one minimum ionizing particle (MIP). At a threshold as low as this, particles passing without interaction were detected, along with nuclear interactions; they were rejected during subsequent processing. Noninteracting particles were used to calibrate the electronic system and determine the beam profile.

SCINTILLATION TRIGGER SYSTEM

As noted above, the trigger system of the NUCLEON experiment is expected to have two levels and be capable of detecting both useful and background events. The destination of this system is to process recorded events in order to select useful data and reject background out-of-aperture events and events with a low energy of a primary particle.

The trigger system consists of three double-sided planes of scintillation strips with single- and multichannel photomultiplier tubes (PMTs) used as photodetectors. The trigger planes are located behind the target, in front of the converter, and behind it. The trigger of the first level is generated within 50–70 ns if the signal

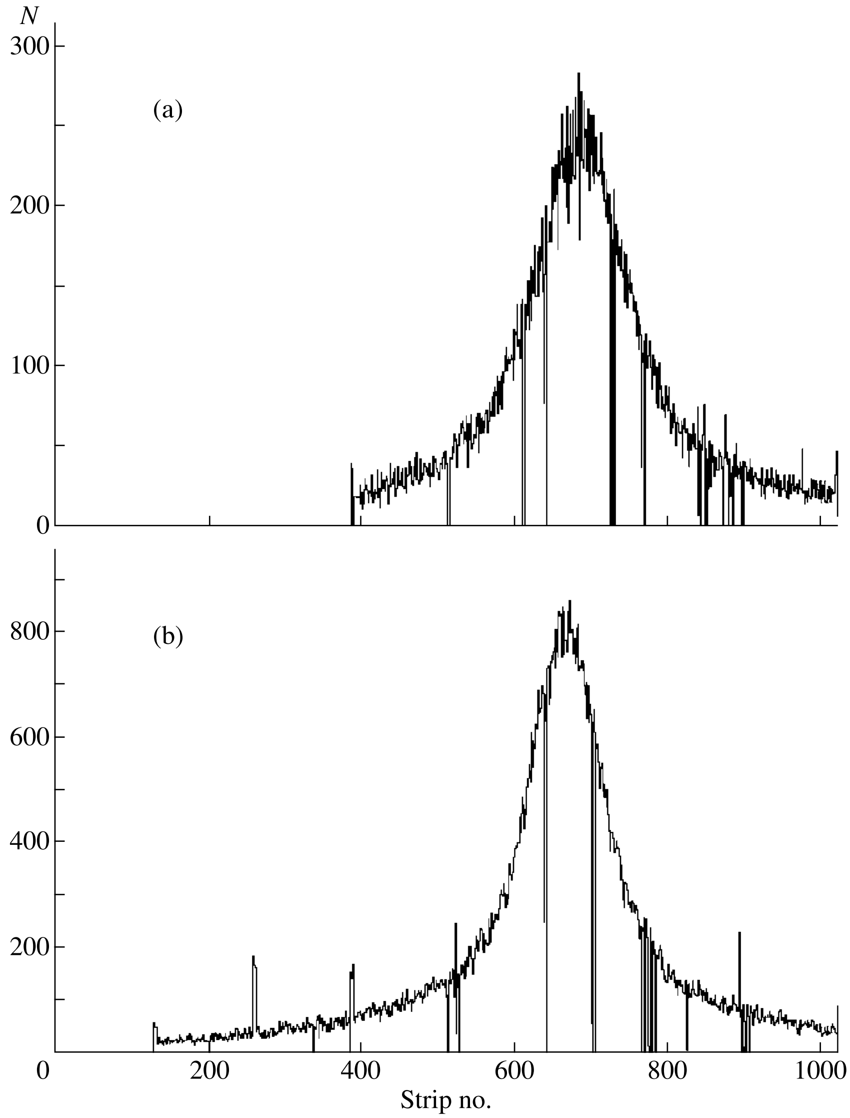

Fig. 5. Profile of the 200-GeV π^- beam obtained in (a) the first and (b) second planes of the strip detectors.

amplitudes in the trigger planes exceed predetermined threshold values. The trigger of the second level is produced upon analyzing the signal amplitudes from individual scintillation strips.

Taking into account that the CR flux in the energy range of 10^{12}–10^{15} eV varies by several orders of magnitude, the thresholds in the first-level trigger can be adjusted to increase the efficiency of selection of rare events at the upper point of the energy range. In addition, the thresholds in the trigger are also governed by the available volume of information that can be transmitted to the Earth, in combination with the possibility of preliminarily filtering the experimental data in an onboard computer.

Four prototypes of multistrip scintillation planes with single-channel R-1355 Hamamatsu PMTs were selected for the high-energy beam tests. Three planes had dimensions of 150 × 150 mm and consisted of 16 strips with a cross section of 10×5 mm^2, and the fourth plane had dimensions of 360 × 360 mm and strips with a cross section of 7.5×5.0 mm^2. The WLS fibers from all strips were combined together and brought out to the photocathodes of each plane's PMTs, so that each the PMTs received a light signal proportional to the total energy deposited in the corresponding plane.

During testing, data were acquired for different variants of the setup configuration and beam parameters. As an example, Fig. 3 shows the distribution of the signal amplitudes from the four planes of the trigger detectors, measured on a 350-GeV pion beam without a target and a converter being installed. Plane SP_1 and scintillation counter S_3 were involved in the trigger system. Based on the test results, we can draw the conclusion that the scintillation planes reliably detect MIPs corre-

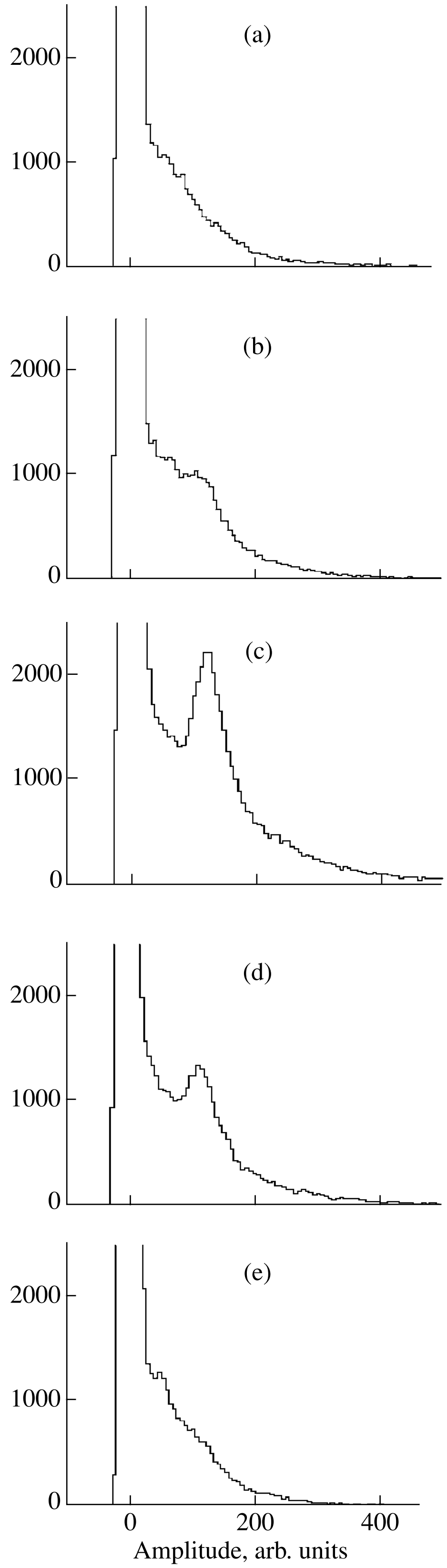

Fig. 6. Amplitude distributions of data from five operating chips of the first microstrip plane: chip nos. (a) 4, (b) 5, (c) 6, (d) 7, and (e) 8. The energy of the π^- beam was 350 GeV.

sponding to the lower limit of thresholds in the first-level trigger and in the mode of trigger system calibration during data acquisition in orbit. The value of the signal amplitude due to an MIP is needed for data analysis.

Analyzing the obtained data, one can estimate the detection efficiencies of planes SP_2 and SP_3, which are 98.32 and 100%, respectively.

The range of pion energies attainable in the test (200–350 GeV) proved to be too small to make an unambiguous inference about the efficiency of event selection by the signal amplitude proportional to the multiplicity. An indirect assessment of the cutoff threshold amplitude can be obtained from comparison to the corresponding distributions (Fig. 4) for a 10-cm-thick carbon target and a 3.5-cm-thick tungsten converter.

SILICON DETECTORS: RESULTS OF THEIR TESTING AND SIMULATION

The main objective of the experimental data processing was to determine whether the prototype of the setup was capable of fulfilling its tasks and whether it was possible, by analyzing its performance, to predict the characteristics of the actual instrument.

To analyze the measured spatial distribution of secondary particles, it is important to know how the primary particles are distributed in the beam and which strips are inoperative. The beam profile obtained in two planes of the strip detector system is shown in Fig. 5. Sharp peaks and dips in the histogram can be attributed to the presence of inoperative strips and to noise induced by the switch during its changeover. After the inoperative strips and noisy channels are excluded from the statistics, one obtains the actual pattern of the spatial distribution of particles in the beam. It is apparent that a larger portion of the beam intensity in both planes corresponds to the fifth to seventh chips; therefore, their characteristics are most essential for further processing.

When converting from the signal amplitude to the number of secondary particles per strip, it is necessary that signal amplitude from minimum-ionizing particles *MIP* in the strip detectors be determined beforehand. However, the presence of a great number of channels (in particular, inoperative channels) makes determination of *MIP* difficult. The amplitude distributions for five operative chips of the first microstrip plane are presented in Fig. 6, and similar distributions for seven operative chips of the second plane are shown in Fig. 7. From the plots, it is apparent that the signals from the detector chips located at the center of the beam with an amplitude equal to *MIP* are clearly distinguishable against the background noise and their values are 120–140 ADC samples in the first plane and ~90 samples in

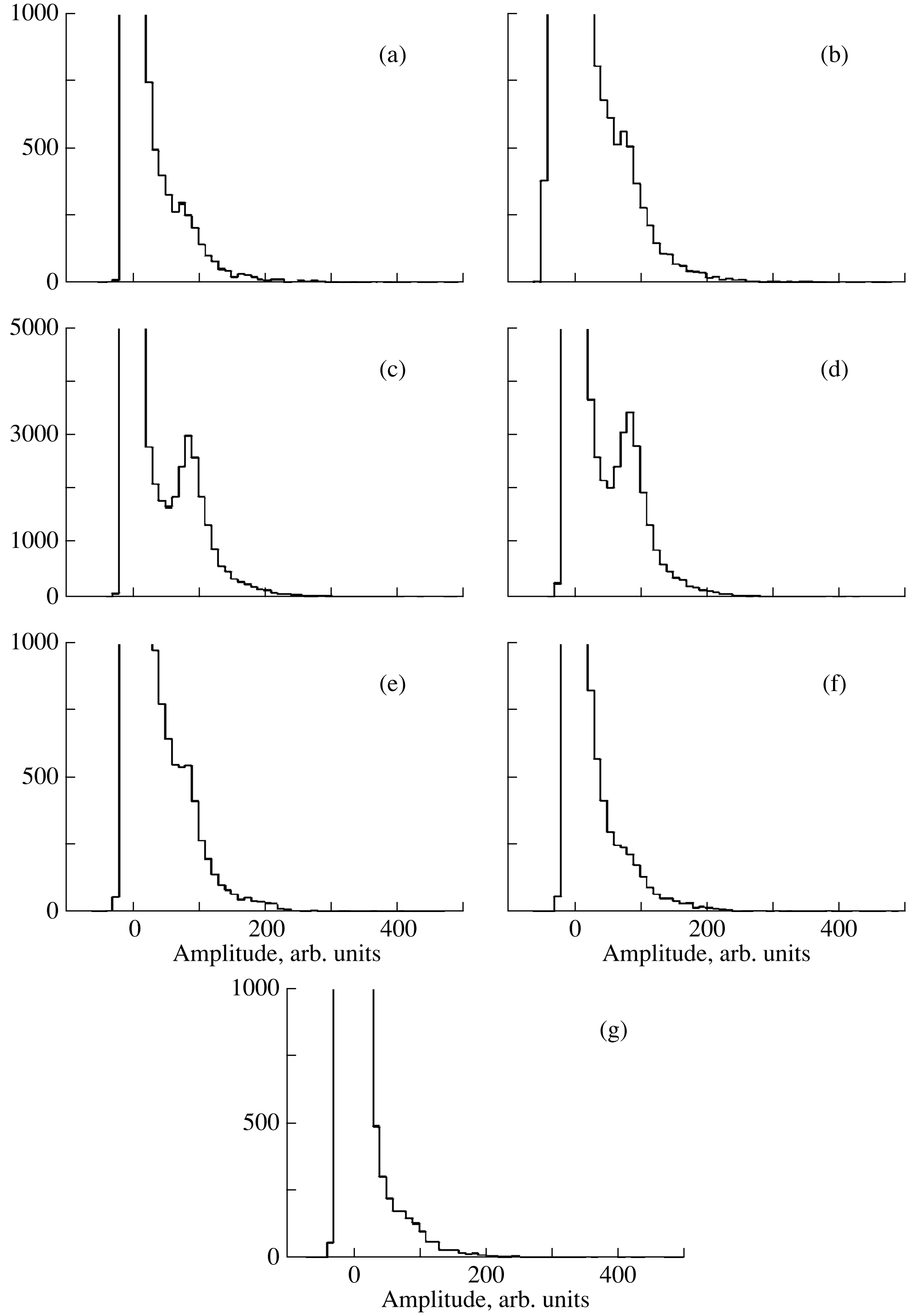

Fig. 7. Amplitude distributions of data from seven operating chips of the second microstrip plane: chip nos. (a) 2, (b) 3, (c) 4, (d) 5, (e) 6, (f) 7, and (g) 8. The energy of the π^- beam was 350 GeV.

the second plane, depending on the chip number. From this point on, when analyzing data from all operative chips of the first plane, the *MIP* value is assumed to be 120; for the second plane, it is equal to 90. This is a good approximation for further processing.

The *MIP* value was also determined to check the charge-measuring system. The amplitude distribution of signals from the second channel of the charge-measuring system is shown in Fig. 8. From the histogram, it is evident that the mean value of *MIP* for this channel

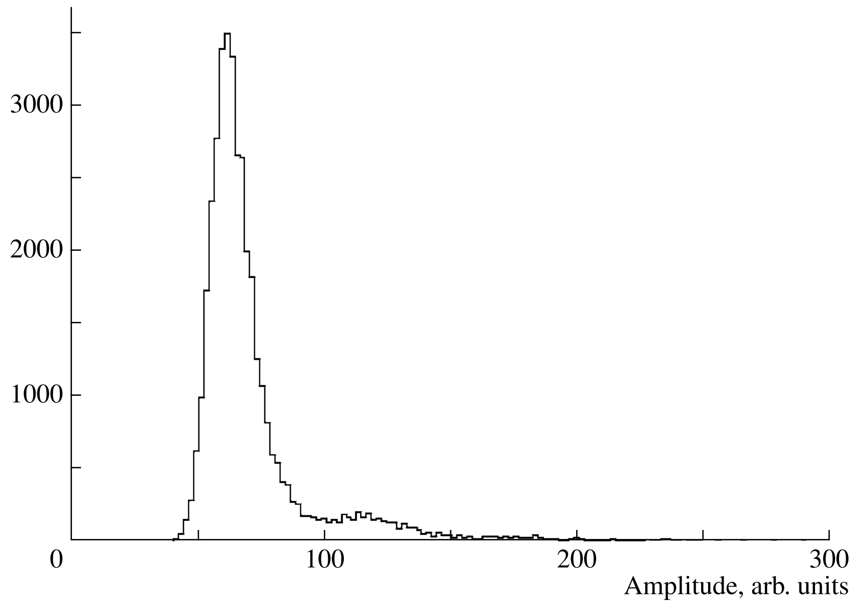

Fig. 8. Amplitude distributions of data from the second channel of the charge-measuring system (π^-, 350 GeV).

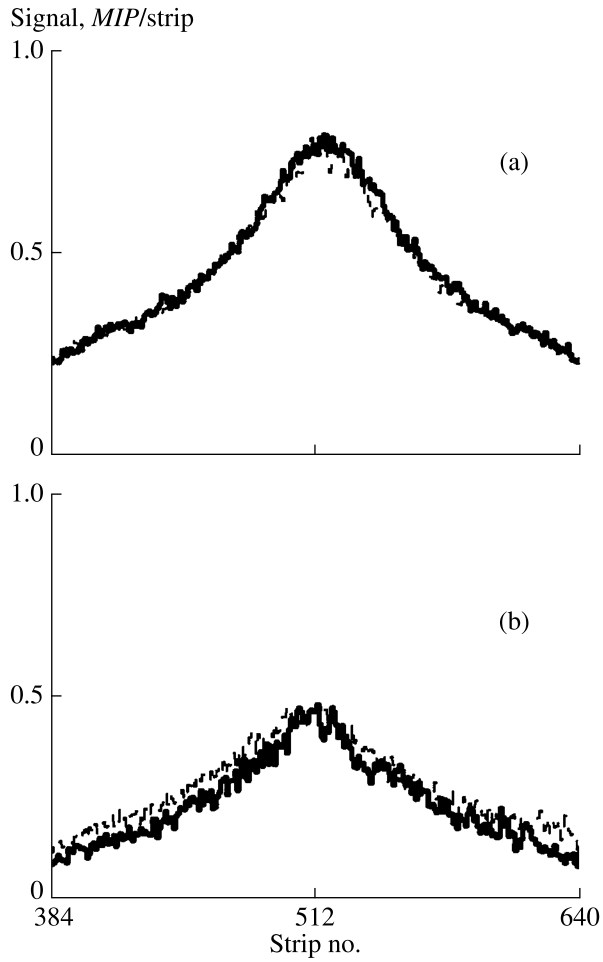

Fig. 9. Spatial distributions of the ionization behind the 10.5-mm-thick tungsten converter for primary pions with energies of (a) 350 and (b) 200 GeV. The experimental data and results of simulation are shown with solid and dashed lines, respectively.

is 60 ADC samples. The presence of peaks corresponding to two MIPs or more is explained by simultaneous passage (with a certain probability) of at least two particles through the detector plane.

As the experimental data were processed, the experiment was simulated using the GEANT 3.21 software package [3]. The ionization loss in each strip was determined during simulation. However, since the parameters of the electronic noise of the equipment were a priori unknown, they were taken into account during processing.

The earlier analysis revealed the necessity of localizing the primary interaction point in order to sort events by the point of the first inelastic interaction (in the target or in the converter) [1]. In the actual setup, this will be done by a separate detector. Among the configurations of the equipment used in the experiment, the one depicted in Fig. 1b is best suited to perform this task. In this variant of the setup, one of the silicon microstrip detectors is located between the target and the converter. Since this variant most closely approximates the actual equipment, it is considered to be the basic one.

Analysis of data obtained in the course of the experiment is hampered by a number of factors: the performance quality of the electronic system, the presence of inoperative strips, and the escape of some particles from the microstrip detectors when the beam is incident on the peripheral region of the setup. Therefore, to select events by the first interaction point and reconstruct the primary energy, the cascade axis must be localized in a transverse plane. Under conditions of a

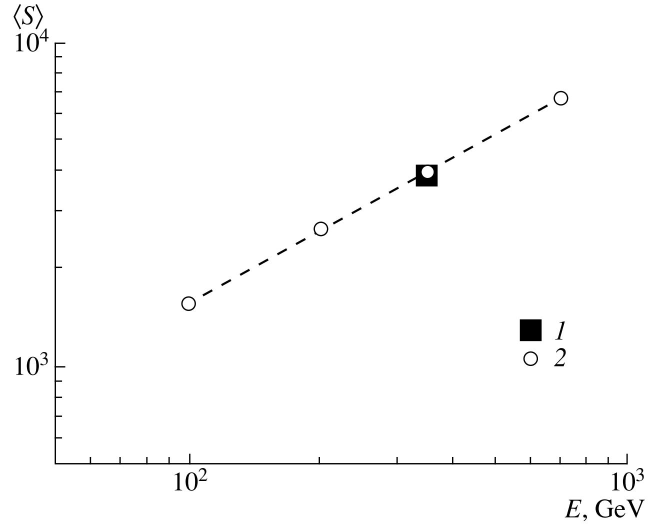

Fig. 10. Calibration curve $\langle S(E)\rangle$ (the tungsten converter was 10.5 mm thick, and the primary particles were pions): (*1*) experiment and (*2*) simulation. A dashed line also presents the simulation results.

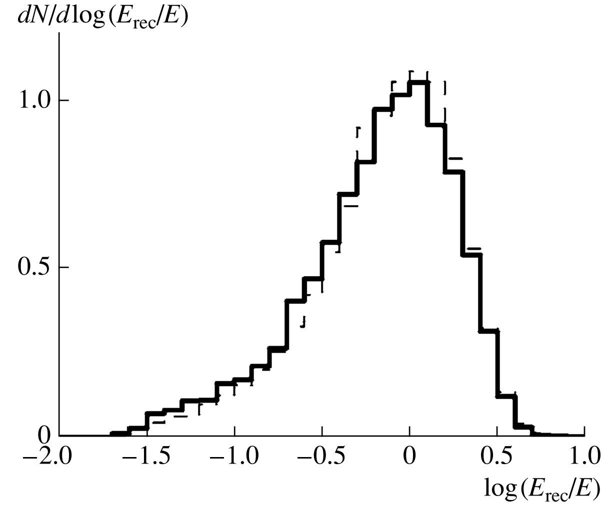

Fig. 11. Distribution in the reconstructed energy (the tungsten converter was 10.5 mm thick, and the primary particles were 350-GeV pions). The solid line presents the experimental data ($\langle E_{rec}\rangle$ = 334 GeV, σ = 0.79), and the dashed line shows the simulation results ($\langle E_{rec}\rangle$ = 350 GeV, σ = 0.78).

developed cascade, this axis can easily be localized with a sufficient accuracy, whereas localization at the initial stage requires that a number of problems be taken into account. First, the particles are few in number, and their spatial distribution fluctuates appreciably. Second, the reverse current background is superimposed on the signals due to these particles. Third, the electronic noise of the equipment produces additional fluctuations.

The method for determining the energy by the spatial density of secondary particles involves, apart from measuring the density itself, determination of the cascade axis with a high accuracy, which turned out to be a difficult task due to the above causes.

A search for a maximum ionization loss in a band of 256 strips was assumed to be the basis for the localization algorithm. Then, the weighted average value of the ionization distribution in the selected band was calculated. The presence of inoperative strips was allowed for when applying the developed algorithm to the simulation data. Simulation of inoperative strips allowed us to take into account the dependence of the accuracy in reconstructing the cascade axis on the particle hit point. When the axis fell into the region with a great number of inoperative strips, this event was excluded from consideration.

Further analysis of both the results of simulation and the experimental data required that the values of ionization per strip be converted into the particle density. The averaged spatial distributions of the particle density were measured using the microstrip detector located past the converter. These distributions obtained for the variant of the setup corresponding to Fig. 1b are shown in Fig. 9. The axis was drawn toward the center of the array in accordance with the described algorithm. It is apparent that simulation reproduces the experimental spatial distribution of secondary particles in the variant of configuration approximating the actual setup.

The correspondence of the calculated spatial distribution of particles to the experimental curve confirms proper selection of the simulation process and the procedures for calibrating the channels against the *MIP* value, finding the shower axis, and measuring the density of particles that hit the strip detectors. A good agreement is observed at different thicknesses of the target and the converter.

The procedure for reconstructing the particle energy comprises the algorithms for obtaining the theoretical calibration dependence of parameter $\langle S(E)\rangle$, approximating it by power dependence $\langle S\rangle \sim E^{\beta}$, determining parameter β, and ascribing measured energy $E_{rec} = aS^{1/\beta}$ to each particle. To obtain the calibration dependence (for the variant closest the actual geometry of the experiment with a tungsten converter 10.5 mm thick), databanks of simulated events were acquired for beam energies of 100, 200, 350, and 700 GeV using the GEANT 3.21 program. Based on these data, the calibration dependences of the mean value of parameter $\langle S(E)\rangle$ were plotted and the index of power was found to be $\beta = 0.75$. Unfortunately, we succeeded in marking only one point $\langle S\rangle$ on this dependence at an energy of 350 GeV for this variant of geometry; nevertheless, it coincided with the theoretical point (see Fig. 10). Using this calibration dependence, reconstructed value of energy $E_{rec} = aS^{1/\beta}$ was assigned to each particle and distributions $\log(E_{rec}/E)$ were plotted. The distributions in the reconstructed energy for a primary pion with an energy of 350 GeV are shown in Fig. 11. The mean energy measured using this technique is $\langle E_{rec} \rangle$ = 334 GeV, and the rms deviation is $\sigma = 0.79$; from the simulation results, we have $\langle E_{rec} \rangle$ = 350 GeV and σ = 0.78. Since the shape of the distribution is highly sensitive to the type of the calibration dependence, the agreement between the measured distribution and the results of simulation indicates that the selected technique is suitable not only for 350 GeV, but for the other energies as well.

CONCLUSIONS

The testing of the particle energy determination technique on the accelerated particle beams with predetermined energies has confirmed the validity of the energy reconstruction algorithm and the efficient operation of the experimental setup prototype. The test results have demonstrated the feasibility of performing an orbital experiment with the proposed equipment.

ACKNOWLEDGMENTS

This work was supported by the Russian Foundation for Basic Research, grant nos. 05-02-16781-a and 05-02-16783-a.

REFERENCES

1. Korotkova, N.A., Podorozhnyi, D.M., Postnikov, E.B., et al., *Yad. Fiz.*, 2002, vol. 65, no. 5, p. 884 [*Phys. At. Nucl.* (Engl. Transl.), vol. 65, no. 5, p. 852].
2. Bashindzhagyan, G.L., Voronin, A.G., Golubkov, S.A., et al., *Prib. Tekh. Eksp.*, 2005, vol. 48, no. 1, p. 46 [*Instrum. Exp. Tech.* (Engl. Transl.), vol. 48, no. 1, p. 32].
3. *GEANT User's Guide. CERN DD/EE/83/1*, Geneva, 1983.
4. Kalmykov, N.N. and Ostapchenko, S.S., *Preprint of Institute of Nuclear Physics, Moscow State University*, Moscow, 1998, no. 98-36/537.
5. Kalmykov, N.N., Ostapchenko, S.S., and Pavlov, A.I., *Nucl. Phys. B (Proc. Suppl.)*, 1997, vol. 52, p. 17.
6. Voronin, A.G., Grebenyuk, V.M., and Karmanov, D.E., *Prib. Tekh. Eksp.*, 2007, no. 2, p. 50 [Instrum. Exp. Tech. (Engl. Transl.), no. 2, p. 187].
7. Tocker, O., Masciocchi, S., Nygard, E., et al., *Nucl. Instrum. Methods Phys. Res., Sect. A*, 1994, vol. 340, p. 572.